Acta Crystallographica Section B
Structural Science
ISSN 0108-7681

Strategies for the structure determination of endohedral fullerenes applied to the example of $Ba@C_{74}\cdot Co(octaethylporphyrin)\cdot 2C_6H_6$

Karen Friese,[a] Martin Panthöfer,[a] Guang Wu[b] and Martin Jansen[a]*

[a]Max-Planck Institut für Festkörperforschung, Heisenbergstrasse 1, 70569 Stuttgart, Germany, and [b]Department of Chemistry, University of California, Santa Barbara, USA

Correspondence e-mail: m.jansen@fkf.mpg.de

Received 3 June 2004
Accepted 14 June 2004

The structure determination of endohedral fullerenes is complicated because of the high degree of disorder which may affect the different structural components, *e.g.* the endohedral atom/molecule, the fullerene cage and solvent molecules. Even worse, the data-to-parameter ratio and, in particular, the scattering power is low. Different strategies are employed to deal with these problems. The observed fraction of the reciprocal lattice may be increased by means of synchrotron diffraction studies. The number of parameters may be reduced by applying rigid-body refinement strategies and by restricting the displacement parameters in the framework of the TLS approach. In the first section, we will give a short overview of the structure determinations of endohedral fullerenes from single-crystal data and discuss the severe problems one may encounter. Then we will give an example of a successful structure analysis of a metal-containing endohedral fullerene, *i.e.* $Ba@C_{74}\cdot Co(OEP)\cdot 2C_6H_6$ (OEP = octaethylporphyrin). Several strategies of refinement, beyond the black box level, have been checked and compared, *e.g.* TLS, split-atom models, twin and single crystal models, anharmonic displacement parameters, and rigid-body models.

1. Introduction

The structure determination of fullerenes in general, and of endohedral fullerenes in particular, is rendered complicated by a series of factors.

Structures containing fullerenes often exhibit a high degree of disorder, which may affect the fullerene cage itself, the endohedral atoms or molecules, and – if present – the solvent molecules. This high degree of disorder implies that the observation of diffraction intensities of the corresponding crystals is limited to low diffraction angles. As a consequence, the resolution of the data is generally not sufficient to resolve *e.g.* the individual C atoms of the fullerene cage.

Different strategies can be employed to overcome these difficulties. At the time of measurement, the use of synchrotron radiation allows a drastic increase in the θ ranges in comparison to those achievable using conventional X-ray sources. In addition, low-temperature scattering experiments further augment the diffraction intensities.

Another consequence of the low resolution of the data is the unfavorable ratio of refinable parameters-to-observed reflections in the structure determination process. It is therefore advisable to introduce symmetry restraints and rigid bodies, respectively, in the refinement process to limit the number of parameters. As has been shown for *e.g.* C_{60} (Bürgi *et al.*, 1993), displacement factor restraints restricting the thermal motions to rigid-body translations and librations (following the strategy developed by Schomaker & Trueblood,

Table 1
Comparison of data for different endohedral fullerenes; OEP = dianion of the octaethylporphyrin.

Compound	*a* (Å) *α* (°)	*b* (Å) *β* (°)	*c* (Å) *γ* (°)	Space group
$Sc_3N@C_{68}\cdot[Ni^{II}(OEP)]\cdot 2C_6H_6$[a]	14.362 (2) 85.433 (2)	14.3902 (14) 88.606 (3)	18.986 (2) 61.786 (3)	$P\bar{1}$
$Sc_3N@C_{78}\cdot[Co(OEP)]\cdot 1.5C_6H_6\cdot 0.3CHCl_3$[b,c]	25.124 (2)	14.9400 (13) 93.720 (2)	19.533 (2)	$C2/m$
$Sc_3N@C_{80}\cdot C_{10}H_{10}O_2\cdot 2C_6H_6$[d]	19.972 (7)	14.196 (5) 117.548 (11)	20.986 (8)	$P2_1/n$
$Sc_3N@C_{80}\cdot 5(o\text{-xylene})$[e]	10.9735 (9) 82.716 (2)	11.1665 (9) 84.728 (2)	14.3101 (11) 80.395 (2)	$P\bar{1}$
$Lu_3N@C_{80}\cdot 5(o\text{-xylene})$[e]	10.9873 (19) 82.747 (3)	11.0872 (19) 84.111 (4)	14.356 (3) 80.741 (3)	$P\bar{1}$
$ErSc_2N@C_{80}\cdot Co^{II}(OEP)\cdot 1.5C_6H_6\cdot 0.3CHCl_3$[f]	25.180 (2)	15.0633 (13) 94.791 (2)	19.650 (2)	$C2/m$
$Er_2@C_{82}\cdot Co^{II}(OEP)\cdot 1.4C_6H_6\cdot 0.3CHCl_3$, isomer 1[g]	17.756 (3) 86.28 (3)	14.818 (3) 86.83 (3)	19.881 (4) 61.74 (3)	$P\bar{1}$
$Er_2@C_{82}\cdot Ni^{II}(OEP)\cdot 2C_6H_6$, isomer 2[h]	14.715 (3) 85.57 (3)	14.799 (3) 86.06 (3)	19.758 (4) 61.82 (3)	$P\bar{1}$
$Ba@C_{74}\cdot Co^{II}(OEP)\cdot C_6H_6$[i]	25.169 (3)	15.018 (3) 93.2 (2)	19.429 (4)	$C2$
Corresponds to a triclinic cell with	14.67 87.2	14.64 87.2	19.439 61.7	

References: (*a*) Olmstead *et al.* (2003*a*,*b*); (*b*) Campanera *et al.* (2002); (*c*) Olmstead *et al.* (2001); (*d*) Lee *et al.* (2002); (*e*) Stevenson *et al.* (2002); (*f*) Olmstead *et al.* (2000); (*g*) Olmstead, de Bettencourt-Dias *et al.* (2002); (*h*) Olmstead, Lee *et al.* (2002); (*i*) this work.

1968) are of further use in order to reduce the number of parameters, while at the same time the anisotropic displacement parameters are kept physically meaningful.

As far as endohedral fullerenes are concerned, a limited number of crystal structure determinations have been reported so far (see Tables 1 and 2). A short overview of the state of the art will be given in the following.

One of the most severe problems encountered in the structure determination of endohedral fullerenes is the strong disorder affecting the endohedral component. So far, this has generally been approximated by split-atom positions with different occupation probabilities. In some cases these reach up to the high number of 23 different sites (Olmstead, Lee *et al.*, 2002; Olmstead, de Bettencourt-Dias *et al.*, 2002) within the fullerene cage. In these particular cases, the refinement of the occupation probabilities of the different split-atom positions was performed with individual, but not identical, displacement parameters. Thus, the significance of the models is at a problematic level and the interpretation suffers from the refinement of counteracting variables.

Similar problems are encountered for the fullerene fragments. A fully ordered fullerene cage, with one single orientation, was encountered only in very few structures (Stevenson *et al.*, 2002; Olmstead, de Bettencourt-Dias *et al.*, 2002). In most cases more than one orientation is observed. Again, the occupation factors for the fullerene cages have been refined without restraining the displacement parameters. The same treatment is also found for the solvent molecules. Furthermore, the refinement of two different types of solvent, *e.g.* benzene and chloroform, on the same position with different occupancies and displacement parameters, as was also carried out by Olmstead, de Bettencourt-Dias *et al.* (2002), Olmstead *et al.* (2001) and Olmstead *et al.* (2000), does not seem to be reasonable.

In addition, some of the triclinic structures determined so far exhibit monoclinic pseudosymmetry with respect to the space group $C2/m$. In the case of $Er@_2C_{82}\cdot Ni^{II}(OEP)\cdot 2C_6H_6$ (OEP = octaethylporphyrin; Olmstead, Lee *et al.*, 2002), a search for missing symmetry leads to deviations from the monoclinic symmetry $2/m$ which are smaller than 0.125 Å. This is a strong indication that the actual symmetry of the compound is monoclinic rather than triclinic. For $Er@_2C_{82}\cdot Co^{II}(OEP)\cdot 1.4C_6H_6\cdot 0.3CHCl_3$ (Olmstead, de Bettencourt-Dias *et al.*, 2002) the deviations from monoclinic symmetry approach 1 Å. The alternatives of higher symmetries and/or twinning, as suggested by the high pseudosymmetry, of either compound have not been discussed.

An additional problem may be related to the non-fullerene part of the structure. In the M^{II}(OEP) co-crystals listed in Table 1 the porphyrin part generally obeys the higher monoclinic symmetry. Apart from the disordered heavy atoms located in the fullerene cage, these molecules represent the dominating part of the diffraction power.

Owing to the effects described above, it is far from trivial to determine the space-group symmetry correctly. Different symmetries have to be checked and the results have to be carefully compared.

In the course of the crystal structure analysis of $BaC_{74}\cdot Co(OEP)\cdot 2C_6H_6$, which was the object of our investigations, we encountered most of the problems described above. In view of the strategies that have been employed for the refinement of endohedral fullerenes up to now, we thought it necessary to give a detailed description of the strategies employed in our crystal structure determination.

2. Structure determination

2.1. Structure solution and preliminary refinement

Single crystals of $BaC_{74}\cdot Co(OEP)\cdot 2C_6H_6$ were synthesized as described in Reich *et al.* (2004). The intensity data of a suitable single crystal were collected at the beamline X3*a*1 at the National Synchrotron Light Source in Brookhaven, New York. For the integration, a triclinic cell with lattice parameters $a \simeq 14.67$, $b \simeq 14.64$, $c \simeq 19.439$ Å, $\alpha \simeq 87.2$, $\beta \simeq 87.2$ and $\gamma \simeq 61.7^\circ$ was chosen.

The structure solution *via* direct methods was carried out with the program *SIR*97 (Altomare *et al.*, 1997) in the two

Table 2
Comparison of data for different endohedral fullerenes.

OEP = dianion of the octaethylporphyrin; NP = number of parameters in the refinement; NR = number of symmetrically independent reflections.

Compound	T (K)	NP	NR	Endohedral	Fullerene	Solvent
$Sc_3N@C_{68}\cdot[Ni^{II}(OEP)]\cdot 2C_6H_6$[a]	91 (2)	1015	19 925	16 Sc sites; 0.25–0.04, 1 N site	3 orientations, 0.5/0.29/0.21	Ordered
$Sc_3N@C_{78}\cdot[Co(OEP)]\cdot 1.5C_6H_6\cdot 0.3CHCl_3$[b]	110 (2)	404	7058	9 Sc sites; 0.50–0.10	2 × 3 orientations 0.25/0.15/0.10	Mixed-occupancy benzene/chloroform
$Sc_3N@C_{80}\cdot C_{10}H_{10}O_2\cdot 2C_6H_6$[c]	91 (2)	985	16 838	2 × 3 Sc sites; 0.95/0.05, 1 N site	Ordered	Ordered
$Sc_3N@C_{80}\cdot 5(o\text{-xylene})$[d]	90 (2)	611	6737	4 Sc sites; 0.5–0.09, 1 N site	Ordered	Partial disorder
$Lu_3N@C_{80}\cdot 5(o\text{-xylene})$[d]	90 (2)	656	6689	22 Sc sites; 0.30–0.01, 1 N site	Ordered	Partial disorder
$ErSc_2N@C_{80}\cdot Co^{II}(OEP)\cdot 1.5C_6H_6\cdot 0.3CHCl_3$[e]	90 (2)	455	6819	4 Sc/Er sites, 1 N site 2 orientations, 0.50/0.50	Mixed-occupancy benzene/chloroform	
$Er_2@C_{82}\cdot Co^{II}(OEP)\cdot 1.4C_6H_6\cdot 0.3CHCl_3$, isomer 1[f]	111 (2)	919	12 169	23 Er sites; 0.35–0.01	Ordered	Mixed-occupancy benzene/chloroform
$Er_2@C_{82}\cdot Ni^{II}(OEP)\cdot 2C_6H_6$, isomer 2[g]	160 (2)	985	9533	23 Er sites; 0.25–0.05	2 orientations, 0.6/0.4	12 C sites partially occupied
$Ba@C_{74}\cdot Co^{II}(OEP)\cdot C_6H_6$[h]	100	97	18 394	2 Ba sites 0.36/0.64	2 orientations 0.46/0.54	Ordered

References: (*a*) Olmstead *et al.* (2003*a*,*b*); (*b*) Campanera *et al.* (2002) and Olmstead *et al.* (2001); (*c*) Lee *et al.* (2002); (*d*) Stevenson *et al.* (2002); (*e*) Olmstead *et al.* (2000); (*f*) Olmstead, de Bettencourt-Dias *et al.* (2002); (*g*) Olmstead, Lee *et al.* (2002); (*h*) this work.

triclinic space groups $P1$ and $P\overline{1}$, and yielded the major part of the porphyrin molecule, as well as part of the C atoms of the fullerene cage. The initial refinement was carried out simultaneously in both space groups with the program *JANA*2000 (Petříček & Dušek, 2000). As the model in $P1$ did not yield better agreement factors than that in $P\overline{1}$, the former space group was discarded. The full experimental details are given in Table 3.[1]

An analysis of the triclinic metrics with the program *LePage* (Le Page, 1982; Spek, 1988) revealed a hidden monoclinic metric according to the transformation: $a_{\rm monoclinic} = a_{\rm triclinic} + b_{\rm triclinic}$; $b_{\rm monoclinic} = a_{\rm triclinic} - b_{\rm triclinic}$; $c_{\rm monoclinic} = -c_{\rm triclinic}$. This suggested either higher symmetry and/or twinning. A twin refinement, assuming the matrix $(0\overline{1}0/\overline{1}00/00\overline{1})$ to describe the twin law, converged at a volume fraction of the two individuals of approximately 0.5:0.5.

On the basis of this result, the twin element was considered to be a real (true) symmetry element. The structure was transformed to the corresponding monoclinic cell with lattice parameters $a = 25.169$ (3), $b = 15.018$ (3), $c = 19.429$ (4) Å; $\beta = 93.3$ (2)°, assuming the space group $C2/m$. At this initial stage, the agreement factors of the monoclinic model were not higher than those of the triclinic one, but the parameter-to-data ratio had improved, considerably. Therefore, the monoclinic symmetry was assumed to be the correct one.

Subsequent refinement cycles and difference-Fourier syntheses in space group $C2/m$ allowed to localize the cobalt-octaethyl-porphyrin molecules as well as benzene molecules (for both molecules H atoms were not taken into account). Additionally, numerous individual C-atom positions, corresponding to part of the fullerene cage, were introduced into the model.

At this point, the difference-Fourier synthesis clearly allowed the identification of the electron density within the fullerene cage, which was assumed to correspond to the endohedral Ba atom. This electron density was arranged close to the mirror plane and we thus placed the cation on a special position at the monoclinic mirror plane. Yet, in subsequent refinement cycles, the anisotropic displacement parameters of the Ba atom exhibited large elongations along the crystallographic b direction. Therefore, it was displaced from the mirror plane and refined as a split-atom position.

Out of approximately 100 maxima in the difference-Fourier synthesis maps, one full C_{74} molecule could be constructed which was oriented in such a way that one of the three vertical mirror planes coincided with the mirror plane of the monoclinic space group. In the beginning the C atoms were treated individually. Yet, due to the high number of parameters necessary to describe this fullerene molecule, the parameter-to-data ratio was disadvantageous for the refinement process and led to unreasonable C—C distances and angles. Therefore, a rigid body was constructed from the results of quantum-chemical molecular structure optimizations of the C_{74}^{2-} dianion (see Reich *et al.*, 2004) and the C_{74} molecule located before was replaced.

To obtain the initial orientation of the model molecule, we retained the individual positions obtained from the difference-

[1] Supplementary data for this paper are available from the IUCr electronic archives (Reference: NA5020). Services for accessing these data are described at the back of the journal.

Table 3
Experimental details.

Crystal data	
Chemical formula	$Ba@C_{74}[Co(OEP)](C_6H_6)_2$
M_r	1774.1
Cell setting, space group	Monoclinic, *C*2
a, *b*, *c* (Å)	25.169 (3), 15.018 (3), 19.429 (4)
β (°)	93.30 (2)
V (Å^3)	7332 (2)
Z	4
D_x (Mg m^{-3})	1.607 (1)
Radiation type	Synchrotron
No. of reflections for cell parameters	1000
θ range (°)	1–17
μ (mm^{-1})	0.63
Temperature (K)	100
Crystal form, color	Rhombic, dark red
Crystal size (mm)	0.04 × 0.04 × 0.02
Data collection	
Diffractometer	Huber four-circle/Bruker Smart 6000 CCD
Data collection method	φ scan, 0.3° per frame, 20 s per frame, φ = 0–360°
Absorption correction	None
No. of measured, independent and observed reflections	18 394, 18 394, 7590
Criterion for observed reflections	$I > 3\sigma(I)$
R_{int}	0.132
θ_{max} (°)	17.0
Range of *h*, *k*, *l*	$-22 \Rightarrow h \Rightarrow 22$ $-11 \Rightarrow k \Rightarrow 13$ $-17 \Rightarrow l \Rightarrow 17$
Refinement	
Refinement on	*F*
$R[F^2>3\sigma(F^2)]$, *wR*, *S*	0.131, 0.186, 2.44
No of reflections	18 394
No. of parameters	97
Weighting scheme	Based on measured s.u.'s; $w = 1/\sigma^2(F)$
$(\Delta/\sigma)_{max}$	0.148
$\Delta\rho_{max}$, $\Delta\rho_{min}$ (e Å^{-3})	1.70, −3.15
Extinction method	B-C type 1 Gaussian isotropic (Becker & Coppens, 1974)

Computer programs used: *SIR*97 (Altomare *et al.*, 1997), *JANA*2000 (Petříček & Dušek, 2000).

Fourier synthesis. We then introduced the model molecule and fixed its orientation with three prominent individual positions. The correctness of the configuration, and the position and orientation of the imported model were confirmed by the close match of the positions of both individual and rigid-body C-atom positions, with a maximum distance of 0.5 Å. Now all the individual C-atom positions were deleted and the coordinates of the center of gravity as well as the angles corresponding to rotations along the monoclinic *b* axis were refined. Only a slight change with respect to the original orientation was observed. As a further test the displacement parameters of the C atoms of the model molecule were refined individually to ensure that each C-atom position corresponded to a maximum in the electron density. No large displacement parameters for any of the C-atom positions were observed and the correct orientation was thus confirmed.

In subsequent refinement cycles, the parameters of the porphyrin and the benzene ring were further refined and the Ba-atom positions were treated as a split atom with anisotropic displacement parameters. At this stage, the difference-Fourier synthesis showed additional peaks, the majority of which nearly centered the positions of the five and six rings of the fullerene cage, indicating the possibility of a second orientation. Although it was not possible to localize a complete second fullerene molecule from the difference-Fourier synthesis, the obtained peaks were still sufficient to define and introduce a second orientation for the C_{74} molecule. A closer inspection of the arrangement of the two fullerene orientations demonstrated that part of the C atoms of the second fullerene corresponded to peaks (found earlier in the difference-Fourier synthesis) that indeed centered the five- and six-membered rings (see Fig. 1). Furthermore, it became obvious that the remaining part of the C atoms of the second orientation could not be identified from difference-Fourier synthesis as they nearly coincide with the positions of the first orientation of the C_{74} molecule.

On the basis of the positions already refined, the OEP molecule was also transformed into a rigid body. In order to limit the number of parameters, the OEP molecule was restricted to the ideal local symmetry 4*mm*. Thus, only the position of the center of gravity, the orientation of the OEP molecule and one isotropic displacement parameter for all C and N atoms of the molecules had to be refined.

2.2. Comparison of different structural models

At this stage of the refinement, the necessity of examining different structural models in detail was evident. A list of the refinements carried out and the corresponding agreement factors is given in Table 4. Hamilton significance tests were

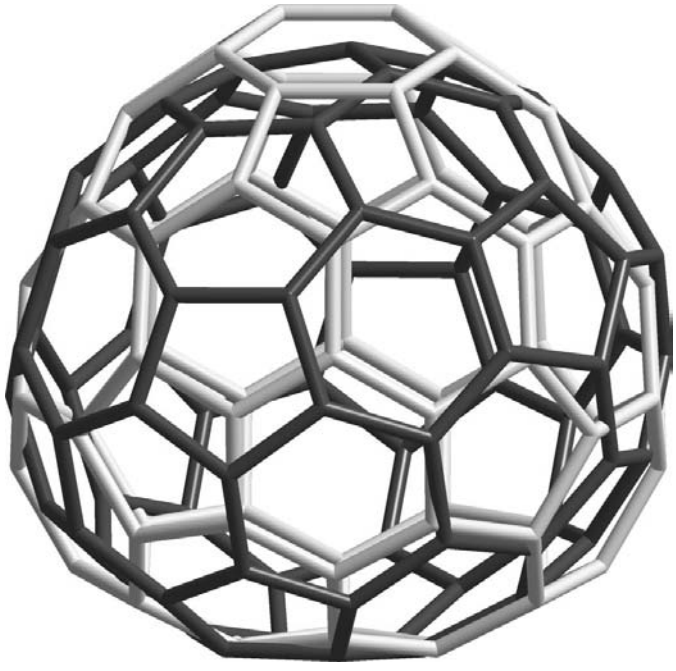

Figure 1
Schematic representation of the two fullerene orientations.

Table 4
Comparison of agreement factors (%) for different refinement models.

Number of reflections in the refinement for all models: 18 394 (7590 > 3σ); N_{par} = number of parameters in the refinement.

Model	Twin		Ba atom	C_{74}	OEP	Benzene	R(obs)	R_w(obs)	R(all)	R_w(all)	N_{par}
1	$C2/m$	–	Split-atom, anisotropic	$U_{iso} = 0.12$	$U_{iso} = 0.054$	$U_{iso} = 0.11$	20.87	24.06	35.76	27.28	56
2	$C2$	1/1	Split-atom anisotropic	$U_{iso} = 0.14$	$U_{iso} = 0.029$	$U_{iso} = 0.08$	19.96	22.51	38.01	25.00	72
3	$C2$	1/2	Split-atom anisotropic	$U_{iso} = 0.14$	$U_{iso} = 0.031$	$U_{iso} = 0.077$	19.89	22.66	37.29	25.08	72
4	$C2$	–	Split-atom anisotropic	$U_{iso} = 0.083$	$U_{iso} = 0.037$	$U_{iso} = 0.077$	14.47	15.92	30.01	19.99	93
5	$C2$	–	One-atom anisotropic	$U_{iso} = 0.070$	$U_{iso} = 0.034$	$U_{iso} = 0.075$	17.78	19.82	35.72	23.37	80
6	$C2$	–	One-atom third-order tensor	$U_{iso} = 0.078$	$U_{iso} = 0.040$	$U_{iso} = 0.084$	16.03	17.91	32.76	21.57	90
7	$C2$	_	Split-atom anisotropic, U_{ij} unrestrained	$T_{ii} = T_{11}, L_{ii}$	T_{ii}, L_{ii}	$U_{iso} = 0.084$	12.74	13.99	26.53	16.91	101
8	$C2$	–	Split-atom anisotropic, U_{ij} restrained	$T_{ii} = T_{11}, L_{ii}$	T_{ii}, L_{ii}	$U_{iso} = 0.072$	13.09	14.55	26.50	18.62	97

carried out in order to compare the individual models (Hamilton, 1964, 1965; Giacovazzo *et al.*, 2002).

First of all, the correct space group had to be identified. For this we compared models where the Ba was treated as a split-atom position with anisotropic displacement parameters (restrained to be equal with respect to the mirror plane). C_{74} was treated as a rigid body with identical isotropic displacement parameters for all the C atoms of the fullerene cage. Both orientations were taken into account. The occupation probabilities for the two Ba positions and the two fullerene cage orientations were allowed to refine. The isotropic displacement parameters of the C atoms of the benzene molecule on one hand and the displacement parameters of the C and N atoms of the octaethylporphyrine molecule on the other hand were restrained to be equal. The OEP was treated as a rigid body with ideal symmetry 4*mm*.

From the preliminary results described above, we were confident that the space-group symmetry was either $C2/m$ or $C2$. The space group Cm was excluded, as the electron density distribution within the fullerene cage indicated the violation of the mirror plane. On this basis, the following structure models were checked: a model in $C2/m$ (model 1 in Table 4), two inversion twin models in $C2$ (model 2 + 3) and a single-crystal model in $C2$ (model 4).

As can be seen from Table 4, the agreement factors in $C2/m$ are significantly higher than in the non-centrosymmetric space group and the Hamilton tests further indicate that $C2$ is the better choice (see Table 5). Furthermore, the single-crystal model in $C2$ is significantly better than the twin models in $C2$.

The main difference in the four models is the treatment of the Ba split-atom positions and the two fullerene orientations. As pointed out above, two Ba-atom positions (termed Ba I and Ba II in the following text) and two possible orientations for the fullerene cage (Ful^{I} and Ful^{II}) were located in the preliminary refinements. In the model in $C2/m$ the two Ba-positions (and the two fullerene orientations) are exactly related *via* the mirror plane (see Fig. 2, left). In the twin models in $C2$ the spatial distribution of the electron density corresponding to the Ba atoms is still strictly restricted *via* the mirror plane, *i.e.* the twin symmetry element, but now the height for the two different positions I and II is determined by the ratio of the twin volume fractions (see Fig. 2, middle). Two different twin models have to be taken into account. In the first one, the scale factor for the Ba position I is equal to the scale factor of fullerene position I, in the second

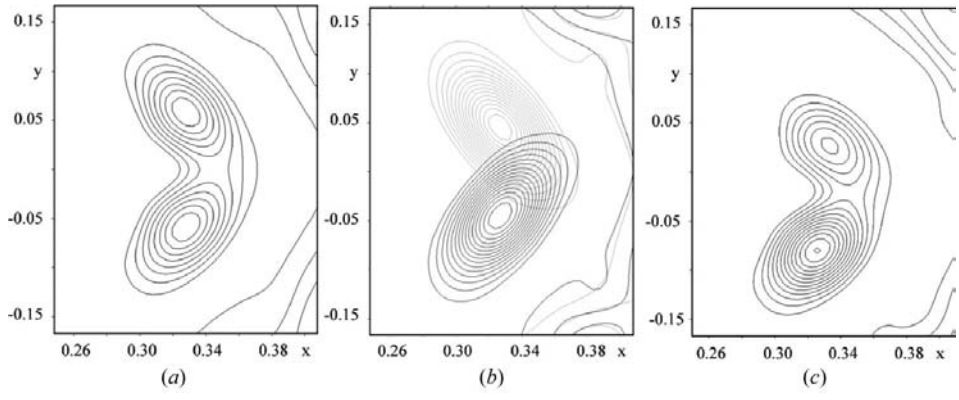

Figure 2
F_{calc} Fourier map around the Ba-atom positions in the different models: (*a*) $C2/m$; (*b*) $C2$ twin models; (*c*) $C2$ single-crystal model.

Table 5
Hamilton tests for the different models.

$T = R_w(\text{obs})/R_w(\text{obs})'$; significance level: 0010. Model B is significantly better than model A, if $T - R > 0.0$.

Pair A–B	T	$F_{b,n-m,a}$	Hamilton (F)	$T - R(F)$
1–5	1.21	1.79333	1.00286	0.21106
5–6	1.11	2.32328	1.00155	0.10510
5–4	1.24	2.13224	1.00185	0.24313
6–4	1.13	3.78423	1.00076	0.12424
2–4	1.41	1.85638	1.00260	0.41135
4–7	1.14	2.51364	1.00134	0.13661
4–8	1.09	3.32167	1.00089	0.09327
8–7	1.04	3.32168	1.00089	0.03914

one Ba position I is restricted to have equal weight as fullerene position II; the weights correspond to the volume fractions of the twin individuals.

In the single-crystal model in space group $C2$, the shape of the electron density is allowed to vary and is no longer restricted with respect to the mirror plane. As can be seen in Fig. 2 (right) the resulting shape of the electron density now deviates clearly from the mirror plane and additionally the heights are not equal any more, displaying a clearly higher electron density at one side of the mirror plane.

The restrictions applied for the two Ba positions and the fullerene cage orientations in the four models can be summarized as follows:

Model 1: $occ_{\mathrm{BaI}} = occ_{\mathrm{FullI}} = occ_{\mathrm{BaII}} = occ_{\mathrm{FullII}} = 0.5$.

Model 2: $occ_{\mathrm{BaI}} = occ_{\mathrm{FullI}} =$ twin volume fraction I;
$occ_{\mathrm{BaII}} = occ_{\mathrm{FullII}} =$ twin volume fraction II;
$occ_{\mathrm{BaI}} + occ_{\mathrm{BaII}} = occ_{\mathrm{FullI}} + occ_{\mathrm{FullII}} = 1$.

Model 3: $occ_{\mathrm{BaI}} = occ_{\mathrm{FullII}} =$ twin volume fraction I;
$occ_{\mathrm{BaII}} = occ_{\mathrm{FullI}} =$ twin volume fraction II;
$occ_{\mathrm{BaI}} + occ_{\mathrm{BaII}} = occ_{\mathrm{FullI}} + occ_{\mathrm{FullII}} = 1$.

Model 4: $occ_{\mathrm{BaI}} + occ_{\mathrm{BaII}} = 1$ and $occ_{\mathrm{FullI}} + occ_{\mathrm{FullII}} = 1$

As the values listed in Table 4 point out, the agreement factors for the models in the non-centrosymmetric space groups are significantly lower than those for the model in $C2/m$. For the two twin models the resulting agreement factors are comparable and the volume fractions are approximately 0.5:0.5. Introducing the occupation probabilities of the two Ba positions and of the fullerene orientations as free parameters into the refinement of the single-crystal model in $C2$ leads to an additional considerable decrease of the overall agreement factor (see Table 4). The superiority of model 4 over models 1–3 was further confirmed by the Hamilton test (see Table 5) and consequently the single-crystal model in $C2$ was chosen as the basis for further refinement.

At this point, the electron density of the endohedral Ba atom had to be approximated in an optimal way. Three different models were checked:

(1) Model 4: two Ba split-atom positions with anisotropic displacement parameters, restricted with respect to the mirror plane

$$u_{11}(Baa) = u_{11}(Bab),\ u_{22}(Baa) = u_{22}(Bab),$$
$$u_{33}(Baa) = u_{33}(Bab),\ u_{12}(Baa) = -u_{12}(Bab),$$
$$u_{13}(Baa) = u_{13}(Bab),\ u_{23}(Baa) = -u_{23}(Bab)$$

(2) Model 5: one Ba atom with anisotropic displacement parameters.

(3) Model 6: one Ba atom described by means of non-harmonic displacement parameters applying a tensor of third order.

As the split atom model proved to be the best (see Tables 4 and 5), this model was applied to the Ba-atom positions in all subsequent refinements.

Until then, the thermal displacement of the atoms of the fullerene cage and the solvate molecule were only very roughly approximated by restraining the isotropic displacement parameters of the light atoms (C,N) to be equal. In order to obtain a physically appropriate description of the electron density distribution corresponding to these molecules, the anisotropic displacement parameters were subjected to purely rigid-body translations and librations in the framework of the *TLS* approach (for details, see Schomaker & Trueblood, 1968). This approach significantly reduces the number of parameters in the refinement process when compared to the use of individual (anisotropic) displacement parameters. On the other hand, it is physically more meaningful than a refinement of isotropic displacement parameters which are restrained to be equal, as it corresponds to the oblate electron density distribution of atoms at the surface of a rotating/librating spherical molecule.

Only the T_{ij} and L_{ij} tensor elements were refined for the two rigid-body molecules; the elements of the S matrix were set equal to zero. While this was straightforward for the octaethylporphyrin, problems were encountered for the refinement of the elements of the T and L tensor of the fullerene cage, which were most probably due to insufficient data quality and the high correlations. Further restraints had to be introduced. First, the diagonal elements of the T tensor were restrained to be equal ($T_{ii} = T_{11}$), while the off-diagonal elements were set equal to zero; second, only the diagonal elements of the L tensor were refined.

As can be seen from Tables 4 and 5, this model (model 8 in the tables) leads to an additional decrease of the agreement factors and the Hamilton test displays it to be significantly better than models 1–6, in which the individual displacement parameters were restrained to be equal.

In addition, we modified model 8 and allowed an individual refinement of the anisotropic displacement parameters of the Ba-atom split positions ($\longrightarrow$ model 7). This led to very different dimensions of the displacement parameters of the two Ba atoms and a strong elongation of the probability density functions. We suppose that this is a consequence of the large correlations introduced into the refinement due to the high pseudosymmetry. The differences in the displacement parameters prevent any reliable information being obtained on the occupancy of the two sites and complicate the crys-

tallochemical interpretation. Despite the better agreement factors for the unrestrained model 7, model 8 is therefore favored.

3. Results and discussion

With respect to the mutual arrangement of the complex units the various models lead to more or less similar results. The final model 8, which we consider to be the best and most informative approximation of the observed electron density, is a single-crystal model in *C*2. In this model the C_{74} fullerene cage and the OEP molecule were restrained to the idealized symmetries of $\overline{3}m$ and 4*mm*, and treated as rigid bodies. The displacement parameters for these rigid bodies were treated using the TLS approach (Schomaker & Trueblood, 1968). Only the elements of the T and L matrix were refined; the elements of the S matrix were set equal to zero. For C_{74}, the diagonal elements T_{ii} of the T matrix were furthermore restrained to be identical.

The displacement parameters of the C atoms of the benzene molecule were restrained to be identical. H atoms were not taken into account.

Two orientations are observed for the fullerene cage (see Fig. 1) with occupation probabilities of 0.46 and 0.54, respectively. The Ba position was treated as a split-atom position; the refined occupancies were 0.36 and 0.64. To keep the occupation factors meaningful, the individual tensor elements describing the displacement parameters of the two Ba positions were restrained with respect to the pseudo-mirror plane.

Fig. 3 shows a projection of the structure of $Ba@C_{74}{\cdot}Co(OEP){\cdot}2C_6H_6$ onto the *a*,*c* plane. For clarity, only one orientation of the C_{74} cage and one Ba position are given; benzene molecules are omitted.

The bond distances and angles observed in the OEP molecule are in good agreement with the literature.

Fig. 4 shows the reconstructed electron density inside the fullerene cage and the corresponding $F_{obs} - F_{calc}$ difference-Fourier synthesis, both calculated on the basis of the final model. One can still see some minor deviations between the observed and calculated model, yet we decided to keep the model at this stage to facilitate the crystallochemical interpretation.

The split-atom distance between the two Ba positions is as long as 1.64 Å, indicating its significant dislocation from the mirror plane. Both positions are shifted considerably from the gravity center of the fullerene cages. The distances are 1.27/1.186 Å for Ba^{I}–$Fu1^{I}$/Ba^{I}–Ful^{II} and 1.23/1.37 Å for Ba^{II}/$Fu1^{I}$ and Ba^{II}/Ful^{II}.

The data quality is not sufficient to obtain reliable information about the possible distortions of the fullerene cage or any deviations from the rigid-body model obtained from the quantum chemical calculations.

The similar lattice parameters of the other OEP-containing endohedral fullerenes (see Table 1) suggest a close relationship between the different crystal structures. Unfortunately, a detailed comparison with the structural models in Olmstead *et al.* (2003*a*,*b*), Campanera *et al.* (2002), Olmstead *et al.* (2001), Lee *et al.* (2002), Stevenson *et al.* (2002), Olmstead *et al.* (2000), Olmstead, de Bettencourt-Dias *et al.* (2002) and Olmstead, Lee

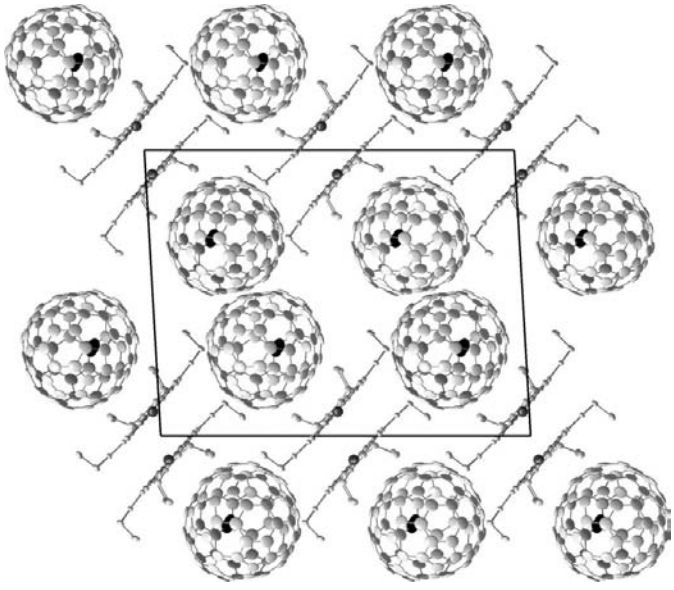

Figure 3
a,*c*-projection of the structure of $Ba@C_{74}COEP{\cdot}2C_6H_6$.

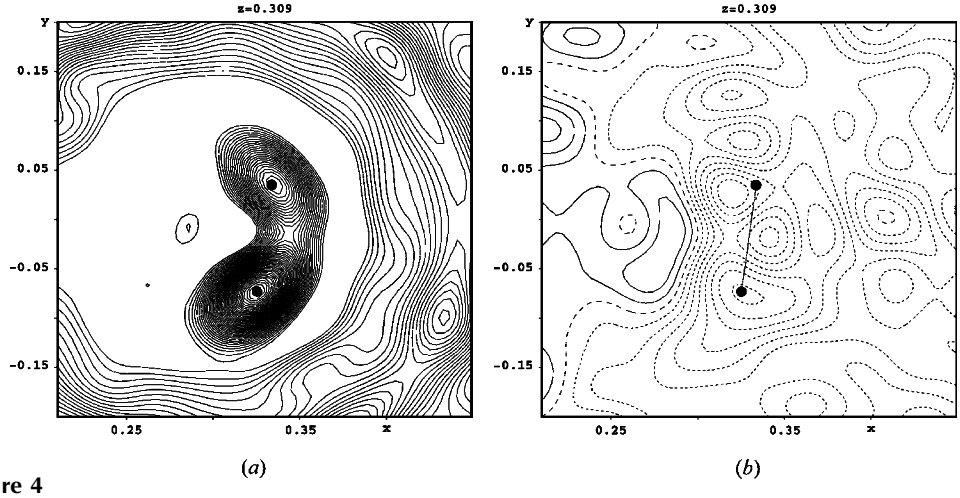

Figure 4
F_{obs} (*a*) Fourier map and (*b*) difference-Fourier map around the Ba-atom positions; reconstructed from the final model. Parameters: center of map = three-dimensional averaged position from the two Ba split-atom positions; 6 Å from the center position in the direction of x, y and z, summed in the direction of z; F_{obs}-map contour definition 5; positive cutoff 212.5; $F_{obs} - F_{calc}$-map contour definition 5; positive cutoff 17.1, negative cutoff 41.1.

et al. (2002) is hardly possible as the refinement strategies applied in these investigation produce ambiguous results.

To conclude, we hope that we have emphasized that the refinement of endohedral fullerenes is by no means a trivial task and it is very difficult to obtain reliable models. Careful investigation has to be carried out to confirm the actual space-group symmetry. Pseudosymmetries of the molecular parts of the structure have to be taken into account. Rigid-body refinement is an absolute need for data sets suffering from such a low resolution and the *TLS* approach is obviously useful to limit the number of parameters in the refinement. The detailed description of the refinement strategies applied in these particular cases may be helpful in future investigations on similar problems.

The authors acknowledge financial support by the BMBF (05 KS1ESA/2). We would like to thank Dr Vaclav Petricek for his continuous support regarding all our questions related to his program.

References

Altomare, A., Cascarano, G., Giacovazzo, C., Guagliardi, A., Moliterni, A. G. G., Burla, M. C., Polidori, G., Camilli, M. & Spagna, R. (1997). *SIR*97. Dipartimento di Geomineralogico, University of Bari, Italy.

Becker, P. & Coppens, P. (1974). *Acta Cryst.* A**30**, 129–147.

Bürgi, H.-B., Restori, R. & Schwarzenbach, D. (1993). *Acta Cryst.* B**49**, 832–838.

Campanera, J. M., Bo, C., Olmstead, M. M., Balch, A. L. & Poblet, J. M. (2002). *J. Phys. Chem. A*, **106**, 12356–12364.

Giacovazzo, C., Monaco, H. L., Artioli, G., Viterbo, D., Ferraris, G., Gilli, G., Zanotti, G. & Catti, M. (2002). *Fundamentals of Crystallography*. Oxford University Press.

Hamilton, W. C. (1964). *Statistics in Physical Science.* New York: Ronald Press Company.

Hamilton, W. C. (1965). *Acta Cryst.* **18**, 823.

Lee, H. M., Olmstead, M. M., Lezzi, E., Duchamp, J. C., Dorn, H. C. & Balch, A. L. (2002). *J. Am. Chem. Soc.* **124**, 3494–3495.

Le Page, Y. (1982). *J. Appl. Cryst.* **15**, 255–259.

Olmstead, M. M., de Bettencourt-Dias, A., Duchamp, J. C., Stevenson, S., Dorn, H. C. & Balch, A. L. (2000). *J. Am. Chem. Soc.* **122**, 12220–12226.

Olmstead, M. M., de Bettencourt-Dias, A., Duchamp, J. C., Stevenson, S., Marciu, D., Dorn, H. C. & Balch, A. L. (2001). *Angew. Chem.* **113**, 1263–1265.

Olmstead, M. M., de Bettencourt-Dias, A., Stevenson, S., Dorn, H. C. & Balch, A. L. (2002). *J. Am. Chem. Soc.* **124**, 4172–4173.

Olmstead, M. M., Lee, H. M., Duchamp, J. C., Stevenson, S., Marciu, D., Dorn, H. C. & Balch, A. L. (2003*a*). *Angew. Chem.* **115**, 928–931.

Olmstead, M. M., Lee, H. M., Duchamp, J. C., Stevenson, S., Marciu, D., Dorn, H. C. & Balch, A. L. (2003*b*). *Angew. Chem. Int. Ed.* **42**, 900–903.

Olmstead, M. M., Lee, H. M., Stevenson, S., Dorn, H. C. & Balch, A. L. (2002). *Chem. Commun.* **22**, 2688–2689.

Petříček, V. & Dušek, M. (2000). *JANA*2000. Institute of Physics, Academy of the Czech Republic, Praha.

Reich, A., Panthöfer, M., Modrow, H., Wedig, U. & Jansen, M. (2004). Submitted for publication.

Schomaker, V. & Trueblood, K. N. (1968). *Acta Cryst.* B**24**, 63–76.

Spek, A. L. (1988). *J. Appl. Cryst.* **21**, 578–579.

Stevenson, S., Lee, H. M., Olmstead, M. M., Kozikowski, C., Stevenson, P. & Balch, A. L. (2002). *Chem Eur. J.* **8**, 4528–4535.